論文

섬유/금속 적층판의 저속 충격 거동

석 우*, 김승현**, 김병선**, 송정일*+

Impact Behavior of Fiber/Metal Laminates (FMLs) under Low Velocity

Yu Shi*, Seung Hyun Kim**, Byung Sun Kim** and Jong Il Song*+

ABSTRACT

The Fiber/Metal Laminates (FMLs) have been developed as a new composite material for aerospace application to reduce weight and improve damage tolerance. In this study, firstly FMLs were manufactured and the tensile test was performed to investigate the mechanical properties of FMLs. Furthermore, impact behavior of the low velocity on FMLs which consisted of different types of aluminum or fiber/epoxy layers was tested by the drop weight impact tester based on the different impact energy conditions. The load-time and energy-time curves were employed to evaluate the impact performance of different specimens. Moreover, finite element analysis (FEA) was also performed to simulate the tensile test and impact behavior of FMLs under the same conditions with the tests and good agreements have been obtained between the FEA predictions and experimental results.

초 록

섬유금속 적층판(FMLs)은 손상허용도를 향상시키고 무게를 줄이는데 적합하여 항공우주 응용의 신소재로 각광을 받고 있다. 본 연구에서는 우선 섬유와 알루미늄을 이용하여 적층판을 제조하여 인장시험을 수행 후 FMLs의 기계적 물성을 평가하였다. 또한 알루미늄과 섬유척층의 변화를 주어 낙추충격시험기(Drop Weight Impact Tester)를 이용하여 저속충격하에서 낙추 높이를 조절하여 각 종류의 시험편 마다 충격시간에 따른 하중과 충격흡수에너지를 각각 비교하였다. 추가로 유한요소해석을 이용하여 시험조건과 동일 조건하 인장과 충격거동해석을 수행한 결과를 실험치와 비교하여 실험과 이론해석이 잘 일치함을 보였다.

Key Words: 섬유금속적층판(FMLs; Fiber/metal laminates), 충격거동(Impact behavior), 저속(Low velocity). 낙추시험기(Drop weigh impact tester), 유한요소해석(Finite element analysis)

1. Introduction

Advanced composite structures offer many advantages when compare with metal alloys, especially where high strength and stiffness to weight ratio is concerned [1]. Aiming this objective, a new lightweight fiber metal laminates (FMLs) have been developed. The FMLs which consist of metal and polymer composite laminates could create a synergistic effect on many properties. The mechanical properties of FMLs show improvements over the properties of both aluminum alloys and composite materials respectively. Carbon fiber/epoxy is tough to be used as an alternative adhesive layer to FMLs, which can be named CARAL (Carbon Reinforced Aluminum Laminates). The combination of high stiffness and strength with good impact property gives CARAL a great advantage for space applications. Other applications for this laminate are impact absorbers for helicopter struts and

* Dept. of Mechanical Engineering, Changwon National University
*+ Dept. of Mechanical Engineering, Changwon National University, corresponding author(E-mail:jisong@changwon.ac.kr)
** Composite Materials Lab, Korea Institute of Materials Science (KIMS)

aircraft seats. Due to its excellent properties, FMLs is chosen to serve as skin material in internal parts of airplanes [2], aircraft lower wing skin [3], and aircraft fuselage [4].

For the aerospace/aeronautical application of the composite laminates, impact performance has been paid more attention by many researchers, especially for the low velocity impact condition. So many published literatures focused the impact analysis on the composite laminates [5-7]. Also a number of researchers have employed the finite element method for the solution of impact on composite laminates. Tan and Sun developed their own finite element program to analyze impact response of composite laminates and they performed impact tests using pendulum type low-velocity impact test system [8].

In this study, mechanical properties of CARAL was investigated by tensile and impact tests. CARAL was tested for tension while 2 groups of specimens were tested by different impact energy under low velociy. Moreover, finite element method is adopted to simulate the tensile and impact tests process using the commercial software ABAQUS 6.7. Finally, load-time and energy-time curves were utilized to evaluate the tested and analyzed results.

2. Experiment and Analysis

2.1 Manufacturing

The most common process used to produce FMLs laminates, as for polymeric composite materials, involves the use of autoclave processing. In this study, there are mainly two steps for the manufacturing of CARAL. Firstly, CFRP was manufactured by the autoclave processing (Fig. 1(a)). Each of CFRP plies is cutting as size of 200 x 700 mm^2. Secondly, adhesive films were inserted between aluminum alloy and CFRP layer. After the lay-up procedure, the specimens were cured in Autoclave machine according to a cure cycle shown in Fig. 1(b).

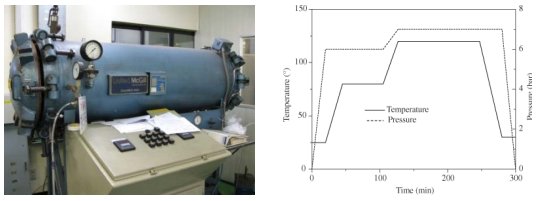

(a) Autoclave machine **(b) Autoclave cure cycle**

Fig. 1 Autoclave cure system for FMLs.

2.2 Tensile test and FE analysis

Static tensile tests were performed in accordance with ASTM D 3039/D3039M-07 [9] which is a tensile test method for tensile properties of polymer matrix composite materials. Referred to the research from Wu and Wu [10], the straight-sided specimen was selected to be used for the tension test of CARAL. Static tensile tests were performed under the servo-hydraulic test frame with a cross-head speed of 2 mm/min at room temperature (Fig. 2). In addition, Al 1050 and CFRP were also tested for the tensile properties.

Tensile test is simulated as the static analysis by the commercial software, ABAQUS V6.7. To simulate the actual specimen, one quarter of straight-sided specimen was modeled due to the symmetric condition. The 3-D modeling with 8-node solid element (C3D8I) and 8-node continuum shell element (SC8R) represented the aluminum and CFRP layers respectively. Elastic-plastic was used to simulate the aluminum material while the homogenized linear elastic orthotropic was applied on CFRP layers.

To simulate the symmetric boundary conditions, the DOF constraints on both of symmetric areas have been fixed as well as the displacement was applied on the tensile direction. FE modeling could be shown as Fig. 3.

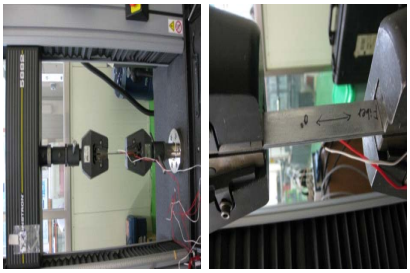

Fig. 2 Tension test machine.

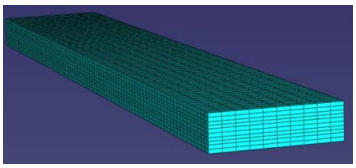

Fig. 3 Finite element model of tensile test.

2.3 Impact test and FE analysis

The low velocity impact tests to 2 different groups of

specimens were carried out. For the tests, drop weight impact tester (R&B Inc., Korea) shown in Fig. 4 was used and embedded measuring device recorded dynamic loading history triggered by velocity sensor of laser beam type while the weighted stainless rigid tup (SS400) start to hit and bounce from a specimen.

All the specimens were 100 × 100mm^2 in size and clamped by an upper steel plate that had a hole with a diameter of 70mm and a lower steel plate that had a hole with a diameter of 30mm. For our impact test, 2 groups of specimens were made as Table 1:

Table 1 Two Groups of specimens for impact tests

Group	CARAL	Aluminum	CFRP
1	CARAL-1	Al 1050 (0.5mm)*3	[0/90/90/0] (0.54mm)*2
	CARAL-2	Al 2024 (0.5mm)*3	[0/90/90/0] (0.54mm)*2
2	CARAL-3	Al 1050 (0.8mm)*3	[0/90/90/0] (0.54mm)*2
	CARAL-4	Al 1050 (0.8mm)*3	[0/45/-45/0] (0.54mm)*2

The dynamic nonlinear transient analysis was simulated for impact tests. The element types of aluminum and CFRP layers are similar with those of tension test. To simulate the circular clamp effect, the modeling of specimen was built as a circular disk shape (Fig. 5), while the nodes at the edge of the model were fixed. The external surface of the hemisphere was simulated as rigid tup, which contacted the central region of the disk. To simulate the actual material behavior, elastic-plastic properties with an isotropic hardening model was applied for aluminum; Orthotropic material was used for CFRP layer in combination with a Hashin damage criteria. SS400 was applied for rigid tup. The impact tests were carried out according to a specification (FD Method) stated in ASTM D 5628-96 [11].

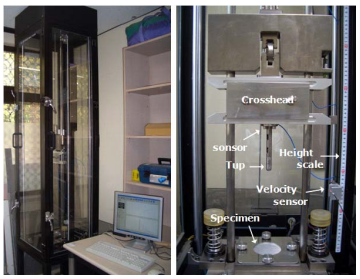

Fig. 4 Drop weight impact tester.

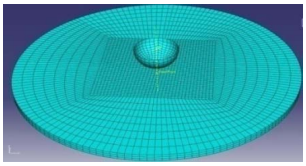

Fig. 5 Finite element model of impact system.

3. Results and Discussions

3.1 Tensile behavior

Fig. 6 shows the tensile stress-strain relations of Al 1050, CFRP and CARAL-3.

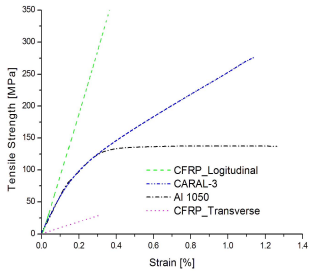

Fig. 6 Stress-strain curves of Al 1050, CFRP and CARAL-3.

It can be seen that Al 1050 exhibits a ductile behavior involving small amount of strain, but CFRP exhibits a brittle behavior while CARAL shows a bilinear stress-strain behavior. It could be known that there are two liner parts in stress-strain curves of CARAL. For the first elastic part, the initial modulus is about 63.71GPa, which is almost the same with that of the initial period of the Al 1050. However, it decreased obviously at a stress level of 75Mpa as shown in Fig. 6. It is because that during the first linear part, both aluminum and carbon/epoxy layers are loaded according to their Young's modulus. After the aluminum starts yielding, the load-carrying capability of aluminum decreased substantially. As a result, the stress-strain curve begins to deviate from the initial linear part, but the stress still increased due to the continued reinforcement of laminate by the carbon/epoxy plies. Beyond the transition region, the stress-strain relation becomes linear again since the carbon/epoxy composite layer typically exhibited a linear elastic response up to ultimate fracture.

Results of FE analysis for simulation of tensile tests can

be shown as Fig. 7. Comparing FEA results with test results, it is almost consistent because the whole material parameters which are obtained from experiments have been used in the analysis process. Thus, it can be known that FE method can simulate the tensile test very well.

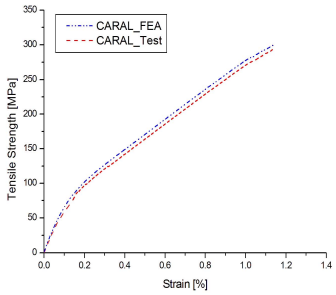

Fig. 7 Stress-strain curves of FE and test results of CARAL-3.

Fig. 8 shows images of scanning electron microscope (SEM) method. It can be shown clearly by SEM that main mechanism damage is delamination between aluminum and CFRP layers. Some fiber breakage and interfacial failure also can be found on CFRP layers.

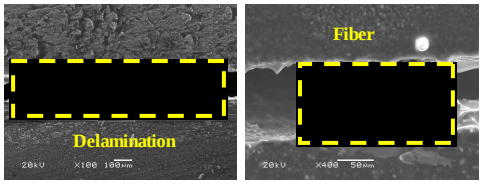

Fig. 8 SEM images of tensile test.

3.2 Results of impact test and analysis

3.2.1 Group 1 (CARAL-1 and CARAL-2)

Fig. 9 shows the load-time curve for CARAL-1, which includes two types of energy levels (2.4J and 9.4J) without any penetration found. For 9.4J of the impact energy levels, it is shown that a maximum impact load of 4.70kN is generated at about 1.6ms, which is the maximum value of peak load compared with other impact tests of other two types of materials. During peak load, some oscillations have been found and it can be explained that the damage may be existed inside the specimen. For 2.4J of the impact energy levels, the peak load is about 2.12kN which happened at 3ms. The contact time is longer than that of impact energy by 9.4J. Also, a rounded shape is shown at the peak which means there is no critical damage area during impact.

The results of FEA could be shown in Fig. 10 (a) and (b), which shows the comparison of experimental and FEA results for impact energy case of 2.4J and 9.4J.

In case of the impact energy of 2.4J, the FEA result shows similar tendency with the experimental result. The peak load from FEA during the impact is higher but the impact time and time to reach the peak load are shorter than the experimental results. The peak load from FEA is about 2.45kN.

In case of the impact energy of 9.4J, the FEA result shows that before reaching the peak load the trend of the curves for both FEA and experiment is almost similar, however, the peak load and time to reach the peak load of FEA are less than those of the experiment. After that, during the post-impact the tendency is similar again.

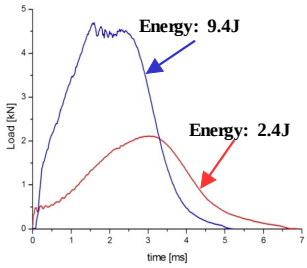

Fig. 9 Impact load-time curve of CARAL-1.

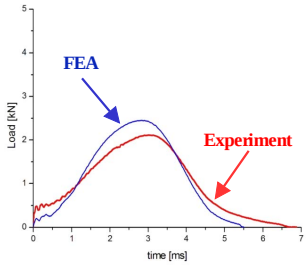

(a) Impact energy of 2.4J

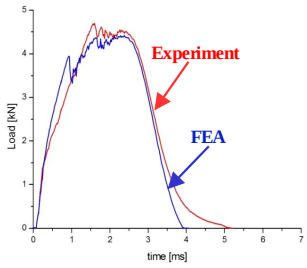

(b) Impact energy of 9.4J

Fig. 10 Comparisons of impact load-time curves of CARAL-1 with experimental and FEA methods.

The discrepancies of the results between FEA and experiment are mainly due to lack of the simulation for adhesive film and failure criteria of aluminum.

Fig. 11 shows the stress distribution from FE analysis for CARAL-1 under two different impact cases. The inner layers of carbon fiber/epoxy prereg could be shown as the smaller figures. Similarly, stress can be distributed as the “peanut shape” contour along the fiber direction compared with CFRP material.

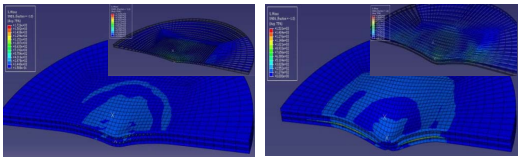

(a) von Mises stress- 2.4J (b) von Mises stress- 9.4J

Fig. 11 Stress distribution of FEA for CARAL-1.

Different from CARAL-1, Al 2024 T3 is used for CARAL-2. Fig. 12 shows the load-time curve for CARAL-2, which includes two types of energy levels (2.4J and 9.4J).

For 2.4J of impact energy level, the shape tendency of load-time curve is a little similar with CARAL-1, however, the maximum impact load is lower (1.84kN) and the contact time (5.4ms) is shorter while time to reach peak load (3.8ms) is later.

For 9.4J of the impact energy level, peak load is 5.21kN at about 3.1ms, which is greater compared with CARAL-1 under the same condition. Also, both of the contact time and time to reach peak load are longer. During peak load, few oscillations could be found for both different cases under the different impact test conditions.

The results of FEA could be shown in Fig. 13 (a) and (b), which show the comparison of experimental and FEA results for impact energy case of 2.4J and 9.4J.

In case of the impact energy of 2.4J, there is a little discrepancy between results of FEA and experimental methods from the beginning of impact happening, the result of FEA is greater than that of experiment. The peak load of FEA during the impact is higher but time to reach the peak load is shorter.

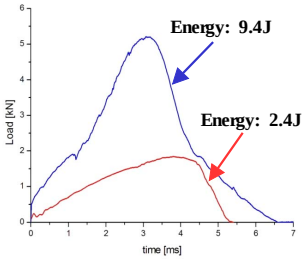

Fig. 12 Impact load-time curve of CARAL-2.

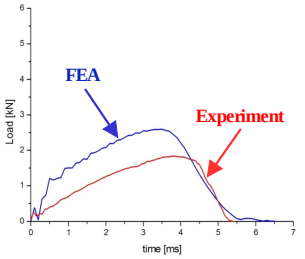

(a) Impact energy of 2.4J

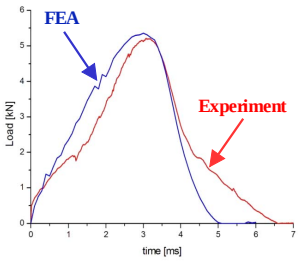

(b) Impact energy of 9.4J

Fig. 13 Comparisons of impact load-time curves of CARAL-2 with experimental and FEA methods.

In case of the impact energy of 9.4J, it is similar compared with FEA and experimental methods although the peak load and time to reach the peak load of FEA are a little higher.

Fig. 14 shows the stress distribution from FEA for CARAL-2 under two different impact cases. Similarly, the stress distribution of carbon fiber/epoxy prepreg could show the “peanut shape” along the fiber direction on each ply, but the area of distribution is smaller compared with the case of CARAL-1, which means the inner damage has been weakened due to the better mechanical properties of Al 2024 T-3.

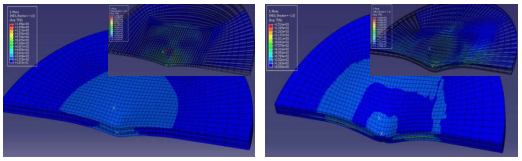

(a) von Mises stress- 2.4J (b) von Mises stress- 9.4J

Fig. 14 Stress distribution of FEA for CARAL-2.

3.2.2 Group 2 (CARAL-3 and CARAL-4)

Fig. 15 shows the load-time curve for CARAL-3, which includes two types of energy levels (2.4J and 9.4J).

For 2.4J of the impact energy level, the shape tendency of load-time curve is a little similar with CARAL-1, however, maximum impact load is lower (2.26kN) and contact time (6ms) is a little shorter. For 9.4J of the impact energy level, similarly, during peak oscillations could be found as damage inside the specimen. The peak load is 5.84kN at about 1.9ms. Also, both of the contact time and time to reach peak load are shorter.

The results of FEA could be shown in Fig. 16 (a) and (b), which show the comparison of experimental and analysis results for impact energy case of 2.4J and 9.4J. In case of the impact energy of 2.4J, the trend of load-time curves from FEA and experiment may be almost similar, the result of FEA is greater than that of experiment. The peak load of FEA during the impact is higher but contact time and time to reach peak load are shorter.

In case of the impact energy of 9.4J, the FEA result shows that the trend of the curves for both FEA and experiment is almost similar at the initial period, however, after that there are some discrepancies existed until the whole impact process has been finished. The discrepancies between the results of FEA and experiment are mainly due to lack of the simulation for adhesive film and failure criteria of aluminum.

Fig. 17 shows the stress distribution from FEA for CARAL-3 under two different impact cases. The stress contour of carbon fiber/epoxy prepreg shows the smaller distributed area compared with results of CARAL-1 due to increase the thickness of aluminum layers.

Fig. 18 shows the load-time curve for CARAL-4, which includes two types of energy levels (2.4J and 9.4J).

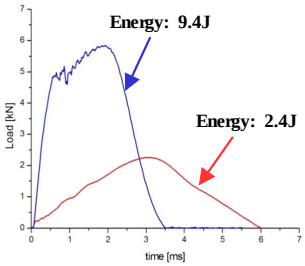

Fig. 15 Impact load-time curve of CARAL-3.

For 2.4J of the impact energy level, the shape tendency of load-time curve is similar with CARAL-3, but the peak of impact load is greater (2.31kN) and contact time (5ms) is a little shorter. Almost a rounded shape could be found at the peak of the curve impacted by 2.4J. For 9.4J of impact energy level, during peak some oscillations have be found and it is indicated that the damage may be existed inside the specimen. The peak load is 5.44kN at about 2.6ms. Comparing with results of CARAL-3, both of the contact time and time to reach peak load are a little longer as well as the peak load is a little lower.

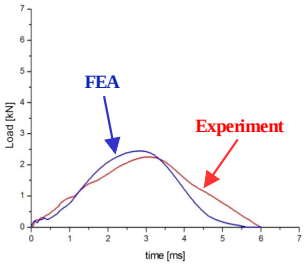

(a) Impact energy of 2.4J

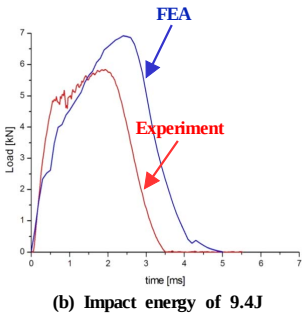

(b) Impact energy of 9.4J

Fig. 16 Comparisons of impact load-time curves of CARAL-3 with experimental and FEA methods.

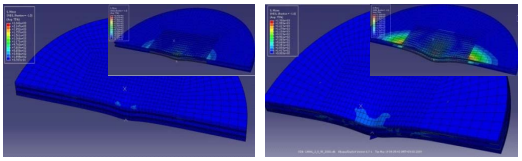

(a) von Mises stress- 2.4J (b) von Mises stress- 9.4J

Fig. 17 Stress distribution of FEA for CARAL-3.

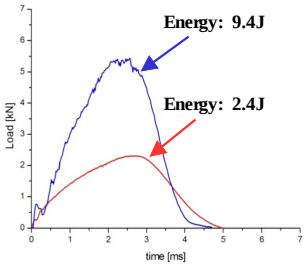

Fig. 18 Impact load-time curve of CARAL-4.

The results of FEA could be shown in Fig. 19 (a) and (b), which shows the comparison of experimental and analysis results for impact energy case of 2.4J and 9.4J.

In case of the impact energy of 2.4J, it is a little different during the initial period between results of FEA and experimental method, the result of FEA is greater than that of experiment. The peak load of FEA during the impact period is higher but the time to reach the peak load is shorter.

In case of the impact energy of 9.4J, from beginning to end of the whole impact, the FEA result shows the different result comparing with the experimental methods. The peak load and time to reach the peak load of FEA are a little higher. However, the tendency of the load-time curve is developed similarly even though the data is somewhat different. The results from FEA also can show some oscillations at the peak as description for damage mechanism of the specimen.

Fig. 20 shows the stress distribution from FE analysis for CARAL-4 under two different impact cases.

3.3 Investigation of impact performance

The impact performances of 2 different groups of specimens are investigated and the results are evaluated by employing the impact energy-time curve.

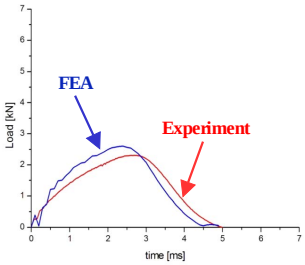

(a) Impact energy of 2.4J

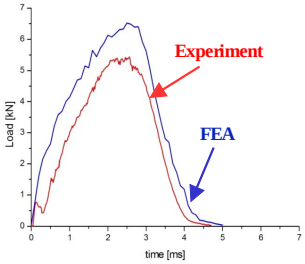

(b) Impact energy of 9.4J

Fig. 19 Comparisons of impact load-time curves of CARAL-4 with experimental and FEA methods.

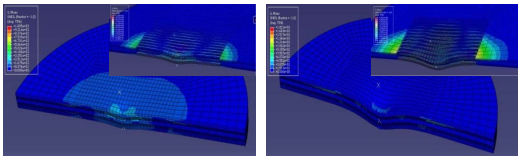

(a) von Mises stress- 2.4J (b) von Mises stress- 9.4J

Fig. 20 Stress distribution of FEA for CARAL-4.

3.3.1 Group 1 (CARAL-1 and CARAL-2)

Fig. 21 shows the energy-time curves for specimens in Group 1.

Fig. 21 (a) shows the energy-time curve of CARAL-1 specimen for two cases of impact energy level. The specimen impacted by 2.4J has absorbed energy of 1.96J, about 18.2% of the impact energy is converted to elastic vibrations or dissipated. The absorbed energy is increased with the increasing of the impact energy, because more failure mechanisms need more energy to achieve. However, the percentage of converted energy is decreased which is about 14.3% because more types of failure mechanisms generated need to absorb more impact energy.

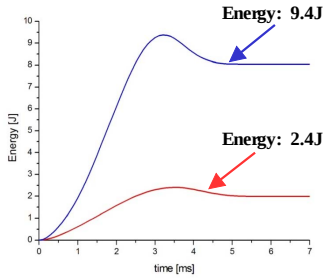

(a) CARAL-1 specimen

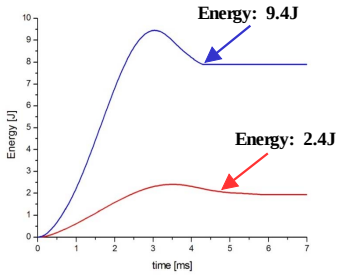

(b) CARAL-2 specimen

Fig. 21 Energy-time curves of Group 1.

Shown in Fig. 21 (b), considering the impact energy of 9.4J, it can be verified that specimens have absorbed energy of 7.87J, so about 16.3% of the impact energy is converted to elastic vibrations or dissipated. However, the specimen impacted by 2.4J has absorbed energy of 1.94J, which is converted 19.2% of the impact energy to elastic vibrations.

To compare with the results of CARAL-1 in Fig. 21(a), it is known that the impact performance of CARAL-2 is better than CARAL-1 due to less energy has been absorbed for damage development during impact process. This is mainly because that the performance of aluminum (Al 2024 T3) of CARAL-2 is better due to other components was involved and some treatments were performed to aluminum, which improves the whole performance of CARAL. Thus, enhancing the mechanical properties of aluminum can improve the impact performance of the whole CARAL.

3.3.2 Group 2 (CARAL-3 and CARAL-4)

Fig. 22 shows the energy-time curves for specimens in Group 2 respectively.

Fig. 22 (a) exhibits the energy-time curve of CARAL-3 for two cases of impact energy level. Considering the impact energy of 2.4J, it can be known that specimens have absorbed energy of 1.77J, so only 26.12% of the impact energy is transferred. However, the specimen impacted by 9.4J has just absorbed energy of 7.68J, which is converted 18.3% of the impact energy to elastic vibrations.

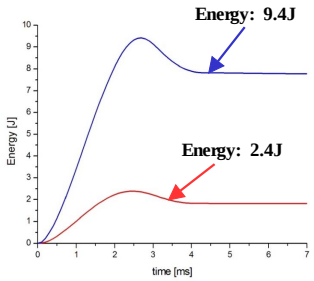

(a) CARAL-3 specimen

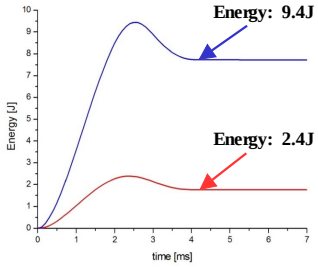

(b) CARAL-4 specimen

Fig. 22 Energy-time curves of Group 2.

Fig. 22 (b) shows the energy-time curve graph of CARAL-4 specimens for two cases of impact energy level. Considering the impact energy of 9.4J, it can be verified that specimens have absorbed energy of 7.76J, about 17.4% of the impact energy is converted to elastic vibrations or dissipated while the specimen impacted by 2.4J has just absorbed energy of 1.83J, which is converted 23.83% of the impact energy as elastic energy. Comparing with results of CARAL-3 and CARAL-4, it is known clearly that the impact performance of CARAL-3 which the stacking sequence of carbon fiber/ epoxy layers is much better than CARAL-4. The main reason is that stacking sequence of CARAL-3 structure is non-symmetric, which can generate a higher residual stress than case of CARAL-4.

4. Conclusions

FMLs have become a new type of composite material which is mainly used on the aerospace industry. Especially, carbon fiber/epoxy layer could be used as an alternative layer to FMLs, which is much lighter and better performance compared with other conventional FMLs such as GLARE (Glass Fiber).

In this study, CARAL was manufactured firstly. After that, some mechanical tests were performed, including the tensile and impact tests. Moreover, FE method was also utilized to simulate the tensile and impact process.

CARAL exhibited a bilinear stress-strain behavior due to effect of aluminum and carbon fiber/epoxy layers by tensile test. FEA also showed the same results with those of experiment.

Impact behavior of FMLs under low velocity was also evaluated by experimental and FEA methods. CARAL have shown better impact performance, especially for the case of higher impact energy. It has been verified that the impact performance of the whole CARAL could be enhanced obviously by improvement of aluminum layers performance. Moreover, CARAL-3 shows the best impact performance due to a non-symmetric stacking sequence in structure which generated a higher residual stress and increased thickness of aluminum layer.

Acknowledgement

This work was partially supported by Brain Korea 21 (BK-21) Projects Corps. of the second phase.

References

1) Choi H. I., “Low-velocity impact analysis of composite laminates under initial in-plane load,” Composite Structrures, Vol. 86, 2008, pp. 251-257.
2) Vlot A. and Gunnink J.W., “Fiber metal laminates,” Kluwer, Delft, 2001, pp. 299-300.
3) Soprano A., Apicella A., D’Antonio L. and Schettino F., “Application of durability analysis to glare aeronautical components,” International Journal of Fatigue, Vol. 18, 1996, pp. 265-272.
4) BotelhoI E.C., Silva R.A., Pardini L.C. and Rezende M.C., “A review on the development and properties of continuous fiber/epoxy/aluminum hybrid composites for aircraft structures,” Material Research, Vol. 9, 2006, No. 10.
5) Abrate S., “Impact of composite laminates,” Applied Mechanics Reviews, Vol. 44, 1991, pp. 155-90.
6) Abrate S., “Impact of laminated composites: recent advances,” Applied Mechanics Reviews, Vol. 47, 1994, pp. 517-44.
7) Abrate S., “Modeling of impacts on composite structures,” Composite Structures, Vol .51, 2001, pp. 129-38.
8) Tan T.M. and Sun C.T., “Wave propagation in graphite/ epoxy laminates due to impact,” 1982, NASA CR 168057.
9) ASTM, “Standard test method for tensile properties of polymer matrix composite materials,” D3039/D3039M-07, 2007.
10) Wu H.F. and Wu L.L., “A study of tension test specimens of laminated hybrid composite. 1: Methods of approach,” Composites Part A: Applied Science and Manufacturing, Vol. 27, 1996, pp. 647-654.
11) ASTM, “Standard test method for impact resistance of flat, rigid plastic specimens by means of a falling fart (Tup or Falling Mass),” D5628-96, 2001.